Supporting Information

Photo-patternable and Stretchable DPP-Based Polymer Semiconductor with Cinnamate Containing Side-Chains

Kaiyuan Chenchai,† Xiaobo Yu,† Cheng Li*, Deqing Zhang*

Table of Contents

1. Materials and measurements

All chemicals were purchased from commercial suppliers and used without further purification unless otherwise specified. Compound **1**[S1] **(Scheme S1)** was synthesized following the reported procedures. **PDPP4T** (Mn / PDI : 49.2 kDa / 1.6) was purchased from Beijing Organtec Ltd.

^{1}H NMR, ^{13}C NMR spectra in solution were recorded at a Bruker AVANCE III 400 MHz spectrometer. High temperature ^{1}H NMR, ^{13}C NMR spectra were recorded at a Bruker Avance III 500WB NMR Spectrometer. Matrix-Assisted Laser Desorption/Ionization Time of Flight (MALDI-TOF) mass spectra were collected on a Bruker Solarix 9.4T FT-ICR mass spectrometer. Elemental analyses were performed on a Thermo Flash Smart instrument. Gel permeation chromatography (GPC) was performed on an Agilent PL-GPC 220 instrument using *o*-dichlorobenzene as an eluent (1.0 mL/min) at 140 °C. Polystyrene was utilized as the calibration standard, and **PDPP4T-CIN** was dissolved in *o*-dichlorobenzene and the concentration was 1.0 mg/mL.

Thermogravimetric analysis (TGA) analyses were carried on a PerkinElmer TGA 8000 Thermogravimetric Analyzer instrument under N_2 at a heating rate of 10 °C/min from 50 °C to 550 °C. UV-vis-NIR absorption spectra were collected on a HITACHI UH4150 UV-Vis spectrophotometer. **PDPP4T-CIN** was dissolved in $CHCl_3$ and the concentration was 5 mg/mL. Thin film was fabricated by spin coating on quartz substrates. Cyclic voltametric (CV) measurements were carried out in a three-electrode cell by using glassy carbon as the working electrode, Pt as auxiliary electrode, and Ag/AgCl (saturated aqueous solution of KCl) as reference electrode on a computer-controlled CHI660C instrument at room temperature; the scan rate was 100 mV/s, and *n*-Bu_4NPF_6 (0.1 mol/L in acetonitrile) was used as the supporting electrolyte. For calibration, the redox potential of ferrocene/ferrocenium (Fc/Fc^+) was measured under the same conditions. HOMO and LUMO energies of this conjugated polymer was estimated with the following equations: HOMO = -(E_{ox}^{onset} + 4.8) eV, LUMO = -(E_{red}^{onset} + 4.8) eV.

Atomic force microscopy (AFM) images were recorded using a Digital Instruments Nano scope IIIa multimode atomic force microscope in tapping mode under ambient conditions. Optical microscope images were recorded using a Leica-DM4M microscope. Two-dimensional grazing-incidence wide-angle X-ray scattering (GIWAXS) measurements were conducted on a Xenocs-SAXS/WAXS system with X-ray wavelength of 1.5418 Å. The thin film samples were irradiated at a fixed angle of 0.2°. The thin films were prepared by spin-coating the **PDPP4T-CIN** solution (10 mg/mL in $CHCl_3$) onto the substrate and thermal annealed at 120 °C for 10

min. The 254 nm light source was generated by Multi-spectrum LED light source purchased from Beijing NBeT Technology Co., Ltd with power density of 300 μW/cm^2.

For the fabrication of bottom-gate/bottom-contact FETs, a n-type Si wafer with a SiO_2 layer of 300 nm and a capacitance of 11.5 nF/cm^2 were used as the gate electrode and dielectric layer, respectively. The gold source and drain bottom electrodes (with Ti as the adhesion layer, *W*/*L* = 1400 μm/50 μm) were patterned by photolithography on a silicon dioxide surface. The substrates were first cleaned with Piranha solution (H_2SO_4: H_2O_2 = 2:1, v/v) for 30 minutes. Then the substrates were further rinsed with deionized water, acetone and isopropanol for three times. After this, the substrates were dried with N_2 and treated with UV ozone cleaning machine for 10 minutes. Lastly, the substrates were placed into a petri dish and one drop of octadecyltrichlorosil (OTS) was dropped into the middle of petri dish. The system was stored under vacuum at 120 °C for 3 h to form an OTS self-assembled monolayer. After the substrate surfaces were modified with OTS, they were washed with $CHCl_3$, hexane and isopropanol sequentially. The polymer solutions were prepared in $CHCl_3$ at a concentration of 5 mg/mL. These solutions were spin-coated onto the OTS-treated Si/SiO_2 substrate at 2000 rpm for 1 min, then thin films with thickness of ca. 40 nm were annealed at 150 °C for 10 minutes. For the patterned thin film, the PDPP4T-CIN film was exposed to UV light with an exposure dose of 300 μW cm^{-2} after the mask was placed on the film. Then, the film was soaked in chloroform for 30 s to remove the unexposed parts. The patterned films were annealed at 150 °C for 10 min. All measuring processes were performed under ambient conditions. It should be noted that the electrical characteristics of polymer FETs are known to be sensitive to atmospheric humidity. In our case, all device tests were carried out during autumn and winter in Beijing, where the relative humidity was consistently low (typically < 10%), which minimizes humidity-induced variability. The FET device performance was evaluated on Keithley 4200 SCS semiconductor parameter analyzer on a probe stage. The calculations of charge mobilities, threshold voltages, on-off current ratios were conducted according to previous report.[S2]

2. Synthesis of PDPP4T-CIN

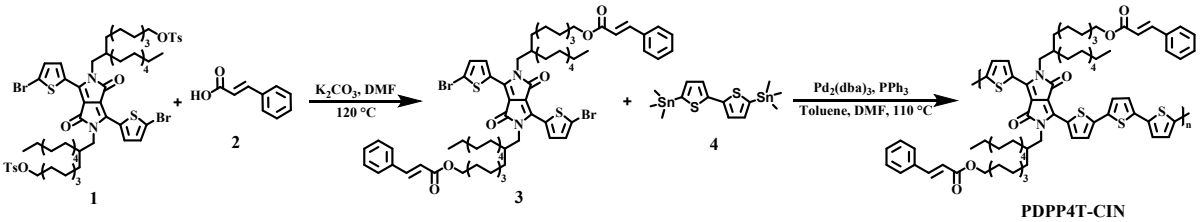

Scheme S1. Synthetic route of **PDPP4T-CIN**.

Synthesis of compound 3

Compound **1** (300.9 mg, 0.22 mmol), compound **2** (130.6 mg, 0.88 mmol) and K_2CO_3 (304.1 mg, 2.2 mmol) were added to a 100 mL double-neck round-bottom flask. 20 mL of dry DMF was injected under nitrogen atmosphere. The reaction was heated to 120 °C and stirred overnight. The reaction was cooled to room temperature. 60 mL of CH_2Cl_2 was added and the reaction was extracted with H_2O for three times. The organic layer was dried with Na_2SO_4. After removal of solvents, the crude product was purified by column chromatography with CH_2Cl_2 and petroleum ether (60-90 °C) (5:1, *v*/*v*). Compound **3** (130.5 mg, 45.6 %) was obtained. ^{1}H NMR (400 MHz, $CDCl_3$): δ = 8.61 (d, 2H), 7.68 (d, 2H), 7.56-7.49 (m, 4H), 7.41-7.34 (m, 6H), 7.21 (d, 2H), 6.44 (d, 2H), 4.18 (t, 4H), 3.92 (d, 4H), 1.92-1.83 (m, 2H), 1.72-1.63 (m, 4H), 1.36-1.18 (m, 60H), 0.87 (t, 6H). ^{13}C NMR (100 MHz, $CDCl_3$): δ = 167.2, 161.6, 144.7, 139.6, 135.4, 134.7, 131.6, 131.3, 130.3, 129.0, 128.2, 119.1, 118.5, 108.2, 64.8, 46.5, 38.0, 32.0, 31.4, 31.3, 30.1, 30.1, 29.8, 29.7, 29.6, 29.5, 29.4, 28.9, 26.4, 26.3, 26.1, 22.8, 14.3, 0.1. HR-MS (MALDI-TOF): calcd. for $C_{72}H_{98}Br_2N_2O_6S_2$ (M^-) 1308.5233; found: 1308.5238. Elemental analysis: calcd. for $C_{72}H_{98}Br_2N_2O_6S_2$: C, 65.94; H, 7.53; N, 2.14; S, 4.89; found: C, 65.84; H, 7.52; N, 2.16; S, 4.95.

Synthesis of PDPP4T-CIN

Compound **3** (60.49 mg, 0.046 mmol), compound **4** (22.54 mg, 0.046 mmol), $Pd_2(dba)_3$ (1.30 mg, 1.37 μmol) and PPh_3 (1.40 mg, 5.49 μmol) were dissolved in 4 mL redistilled toluene in a Schlenk tube. Through a freeze-pump-thaw cycle, the tube was charged with nitrogen for three times. The reaction mixture was stirred at 110 °C for 3.5 h. The mixture was poured into CH_3OH and filtered. Then, the polymer was purified by Soxhlet extraction with various solvents (CH_3OH, acetone and hexane sequentially) to remove the existing oligomers and other impurities. The chloroform fraction was collected. After removal of solvents, and the sample was dried under vacuum at 50 °C for 12 h. **PDPP4T-CIN** was obtained as a deep green solid (55.12 mg, 90.9 %). ^{1}H NMR (500 MHz, 1,1,2,2-tetrachloroethane-d_2, 373 k): δ = 9.02-8.70 (m, 2H), 7.66-7.60 (m, 2H), 7.51-7.45 (m, 4H), 7.37-7.31 (m, 6H), 7.30-6.67 (m, 6H), 6.42-6.37(m, 2H), 4.54-3.59 (m, 8H), 2.09-1.91 (m, 2H), 1.70-1.62 (m, 4H), 1.41-1.23 (m, 60H), 0.89-0.84 (m, 6H). ^{13}C NMR (126 MHz, 1,1,2,2-tetrachloroethane-d_2, 373 k): δ = 166.6, 160.7, 144.3, 141.9, 141.3, 134.8, 130.1, 128.8, 128.0, 118.8, 64.7, 50.9, 31.9, 31.9, 31.8, 31.7, 30.3, 30.2, 30.2, 30.1, 30.1, 30.1, 29.7, 29.6, 29.6, 29.6, 29.5, 29.5, 29.3, 28.9, 26.7, 26.6, 26.0, 22.6, 14.0, 4.3. Elemental analysis: calcd. for $C_{80}H_{102}N_2O_6S_4$: C, 73.02; H, 7.81; N, 2.13; S, 9.75; found: C, 72.47; H, 7.78; N, 1.67; S, 9.57.

3. Gel permeation Chromatography (GPC) curve of PDPP4T-CIN

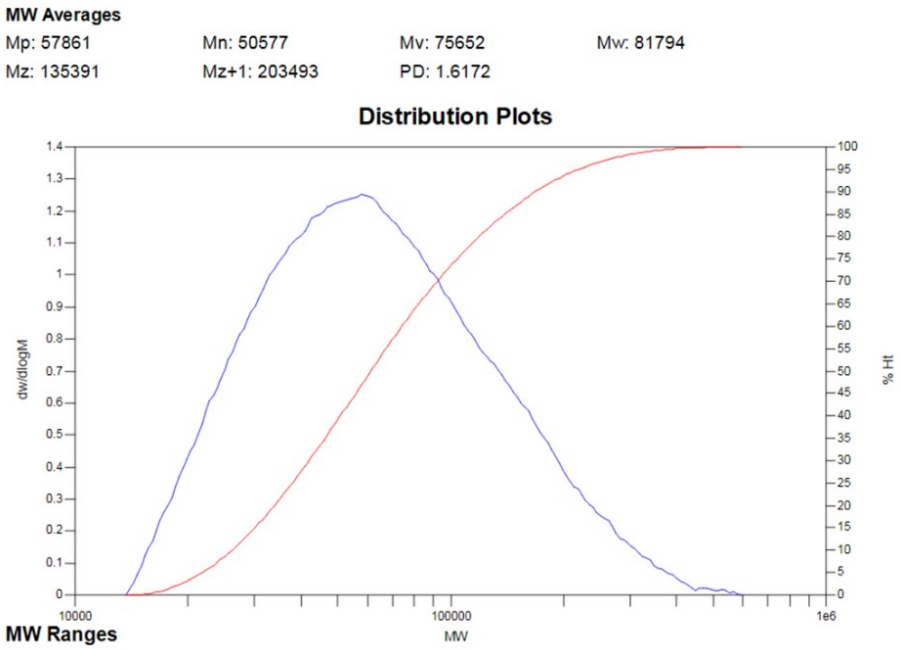

Figure S1. Gel Permeation Chromatography (GPC) curve of PDPP4T-CIN.

4. Absorption spectra and cyclic voltammogram (CV) of PDPP4T-CIN

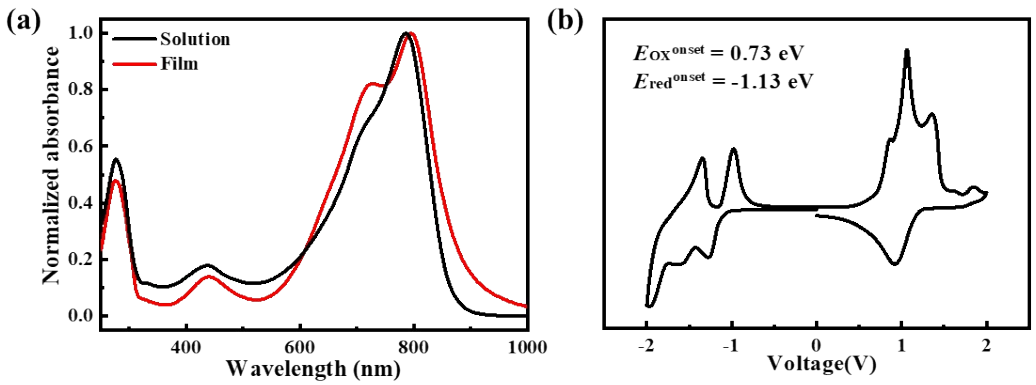

Figure S2. (a) Absorption spectra of **PDPP4T-CIN** in chloroform and its thin film. (b) Cyclic voltammogram of **PDPP4T-CIN**; the scan rate was 100 mV/s; potential vs. Fc/Fc^{+}.

5. Thermogravimetric analysis (TGA) of PDPP4T and PDPP4T-CIN

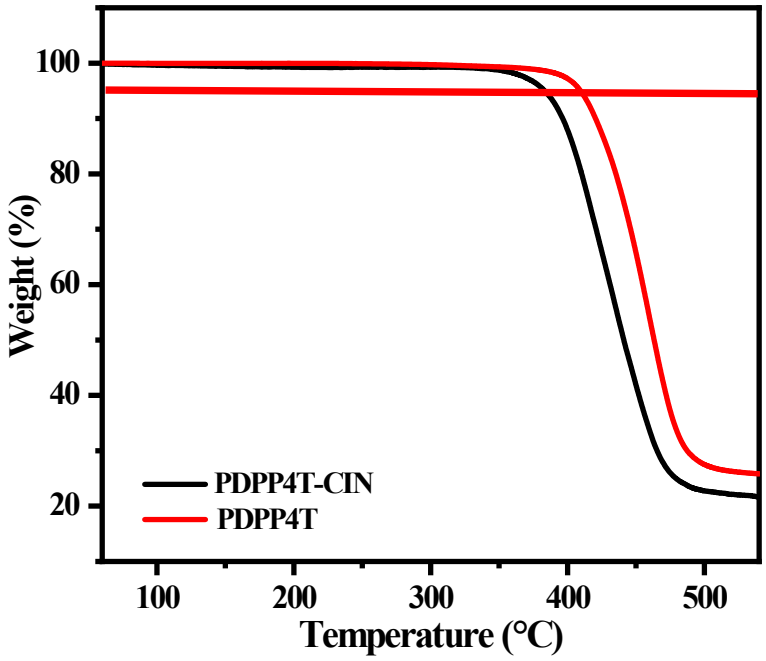

Figure S3. Thermogravimetric analysis curve of **PDPP4T-CIN** and **PDPP4T**; Heating rate: 10 °C/min, from 50 °C to 550 °C under nitrogen atmosphere.

6. Charge transport properties of the devices with the photo-patterned thin film of PDPP4T-CIN

Table S1. Charge mobility, threshold voltage, on/off ratio, etc. for the respective devices with the pristine and photo-patterned thin film of PDPP4T-CIN.[a]

	$\mu_{avg.}$ [$cm^2V^{-1}s^{-1}$]	I_{on} [mA]	V_{th} [V]	I_{on}/I_{off}
Pristine films	1.71 ± 0.09	0.18 ± 0.004	~1.35	~10^4
Photo-patterned films	1.59 ± 0.06	0.17 ± 0.008	~2.06	~10^4

[a] All average mobilities are based on ten independent devices and expressed as means ± standard deciations (SD).

7. Thickness variation of PDPP4T-CIN films

Table S2. Summary of PDPP4T-CIN film thickness measured before and after UV irradiation, solvent development, and thermal annealing.[a]

	As-cast [nm]	After UV irradiation [nm]	After solvent development [nm]	After subsequent thermal annealing [nm]
PDPP4T-CIN	34.6 ± 1.6	34.8 ± 1.6	33.9 ± 1.2	33.5 ± 0.9

[a)] All average thickness are based on five independent films and expressed as means ± standard deciations (SD).

8. The GIWAXS patterns

Table S3. Summary of the *q* values and the corresponding *d*-spacing.

	q value [Å^{-1}]		*d*-spacing [Å]	
	(100)	(010)	(100)	(010)
Pristine thin film	0.24	1.65	26.2	3.81
Photo-patterned thin film	0.26	1.65	24.2	3.81

9. Stretching behavior of crosslinked PDPP4T-CIN thin films

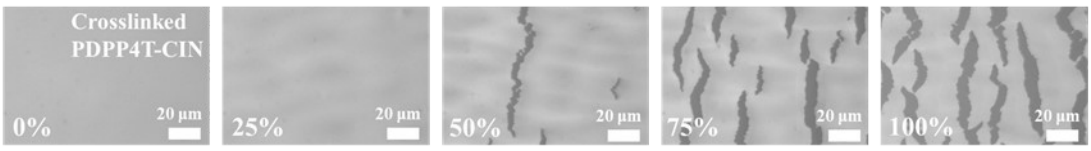

Figure S4. Optical microscopic images of the UV-irradiated films under different strains, scale bar: 20 μm.

10. Charge transport properties of the stretched PDPP4T-CIN thin films

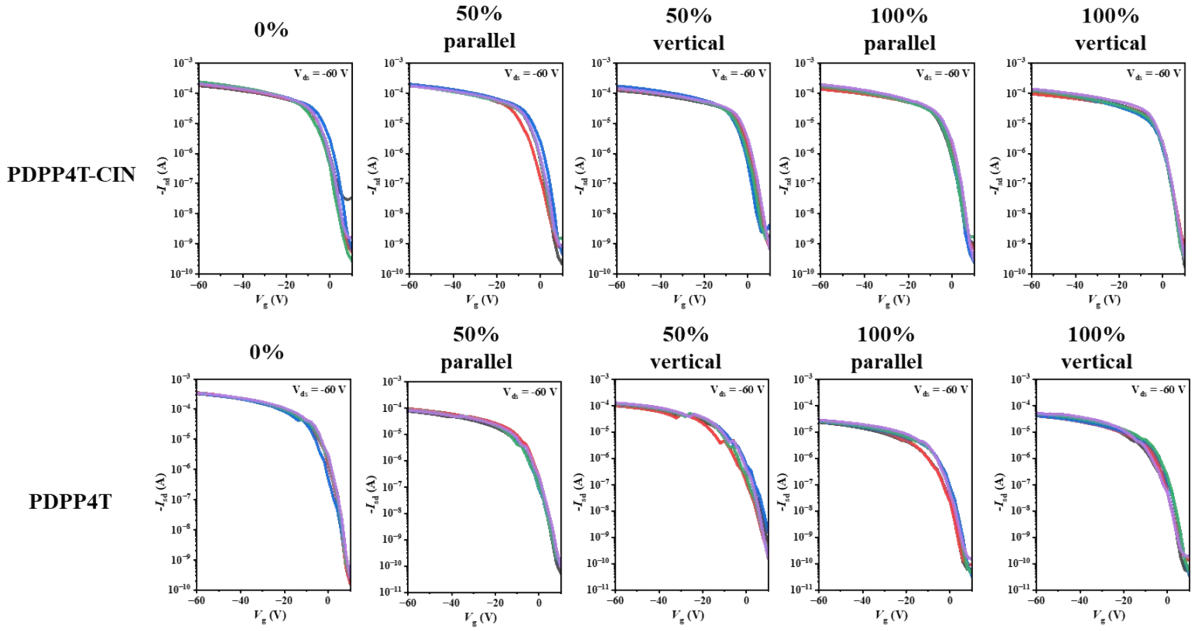

Figure S5. Transfer curves of FETs with stretched thin films of **PDPP4T-CIN** and **PDPP4T** under different strains. Parallel represents charge transporting direction parallel to strain direction, and vertical represents charge transporting direction perpendicular to strain direction.

Table S4. Semiconducting performance data for the devices with the stretched thin films of **PDPP4T-CIN and PDPP4T** under different strains.

Strain		PDPP4T				PDPP4T-CIN			
		$\mu_{avg.}$ [$cm^2V^{-1}s^{-1}$]	V_{th} [V]	I_{on} [mA]	I_{on}/I_{off}	$\mu_{avg.}$ [$cm^2V^{-1}s^{-1}$]	V_{th} [V]	I_{on} [mA]	I_{on}/I_{off}
0%		1.98 ± 0.084	-2.1 ~ 3.3	0.34 ± 0.01	$10^6 \sim 10^7$	1.73 ± 0.082	-1.6 ~ 4.1	0.20 ± 0.02	$10^5 \sim 10^7$
50%	//	0.50 ± 0.035	-2.7 ~ 0.3	0.08 ± 0.007	$10^5 \sim 10^6$	1.60 ± 0.044	-3.2 ~ 2.7	0.18 ± 0.01	$10^5 \sim 10^6$
	⊥	0.64 ± 0.050	-4.8 ~ 0.1	0.11 ± 0.01	$10^5 \sim 10^6$	1.42 ± 0.074	0.3 ~ 3.8	0.14 ± 0.02	$10^5 \sim 10^6$
100%	//	0.11 ± 0.035	-2.9 ~ 1.2	0.02 ± 0.002	$10^5 \sim 10^6$	1.48 ± 0.037	0.9 ~ 2.5	0.16 ± 0.02	$10^5 \sim 10^6$
	⊥	0.20 ± 0.030	-3.5 ~ 1.3	0.04 ± 0.005	$10^6 \sim 10^7$	1.16 ± 0.073	2.2 ~ 3.4	0.12 ± 0.02	$10^5 \sim 10^6$

[a] All average charge mobilities are based on 5 independent devices. //represents charge transporting direction parallel to strain direction, and ⊥represents charge transporting direction perpendicular to strain direction.

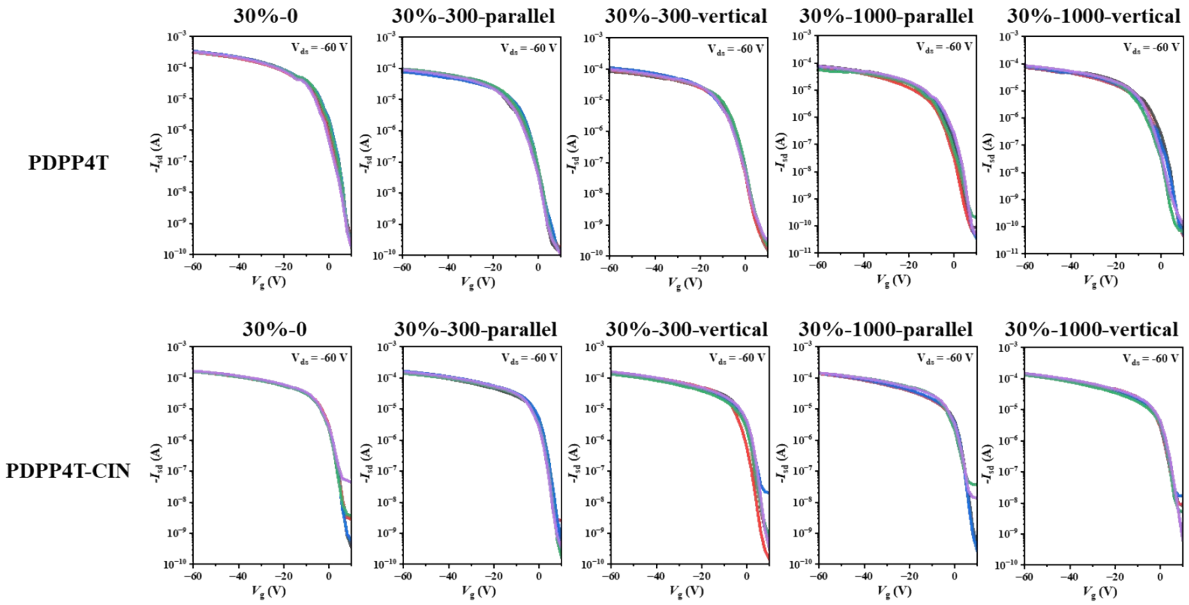

Figure S6. Transfer curves of FETs with **PDPP4T** and **PDPP4T-CIN**, which were separately subjected to cyclic stretching and releasing for 300 and 1000 times under 30% strain. Parallel represents charge transporting direction parallel to strain direction, and vertical represents charge transporting direction perpendicular to strain direction.

Table S5. Semiconducting performance data for devices with the stretched thin films of **PDPP4T-CIN** and **PDPP4T** under 30% stain for different stretching and releasing cycles.

Cycle times		PDPP4T				PDPP4T-CIN			
		$\mu_{avg.}$ [$cm^2V^{-1}s^{-1}$]	V_{th} [V]	I_{on} [mA]	I_{on}/I_{off}	$\mu_{avg.}$ [$cm^2V^{-1}s^{-1}$]	V_{th} [V]	I_{on} [mA]	I_{on}/I_{off}
0		1.70 ± 0.083	-2.1 ~ 2.4	0.32 ± 0.01	$10^6 \sim 10^7$	1.62 ± 0.036	2.3 ~ 2.9	0.16 ± 0.004	$10^5 \sim 10^6$
300	//	0.61 ± 0.036	-4.6 ~ -1.1	0.09 ± 0.007	$10^5 \sim 10^6$	1.58 ± 0.047	2.4 ~ 4.6	0.15 ± 0.01	$10^5 \sim 10^6$
	⊥	0.67 ± 0.045	-3.3 ~ -1.4	0.10 ± 0.01	$10^5 \sim 10^6$	1.44 ± 0.054	0.3 ~ 4.1	0.15 ± 0.009	$10^4 \sim 10^6$
1000	//	0.33 ± 0.031	-2.4 ~ 0.3	0.07 ± 0.009	$10^6 \sim 10^7$	1.46 ± 0.058	2.5 ~ 4.9	0.14 ± 0.003	$10^4 \sim 10^6$
	⊥	0.45 ± 0.066	-4.1 ~ 0.1	0.08 ± 0.005	$10^6 \sim 10^7$	1.35 ± 0.036	3.2 ~ 4.7	0.14 ± 0.006	$10^4 \sim 10^6$

[a] All average charge mobilities are based on 5 independent devices. //represents charge transporting direction parallel to strain direction, and ⊥represents charge transporting direction perpendicular to strain direction.

11. NMR spectra

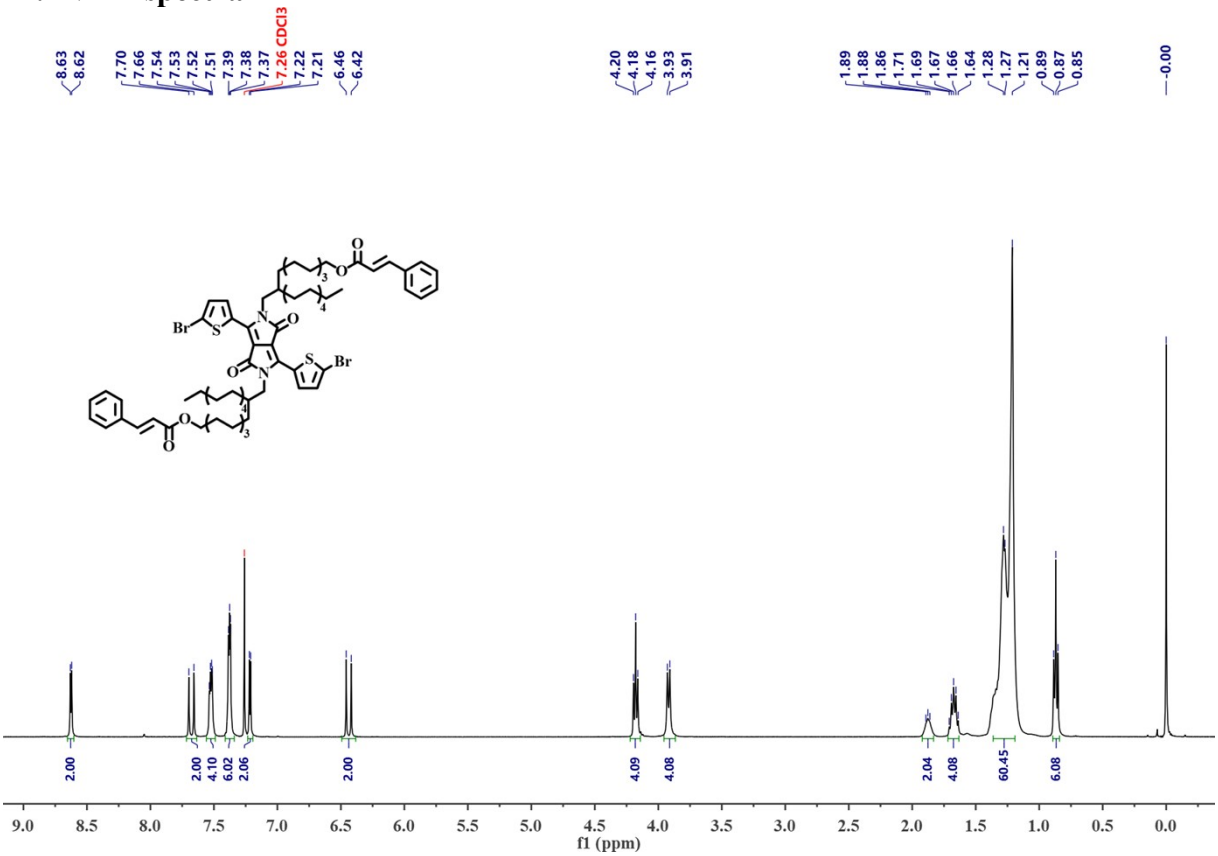

Figure S7. ^{1}H NMR spectrum of **3** in $CDCl_3$.

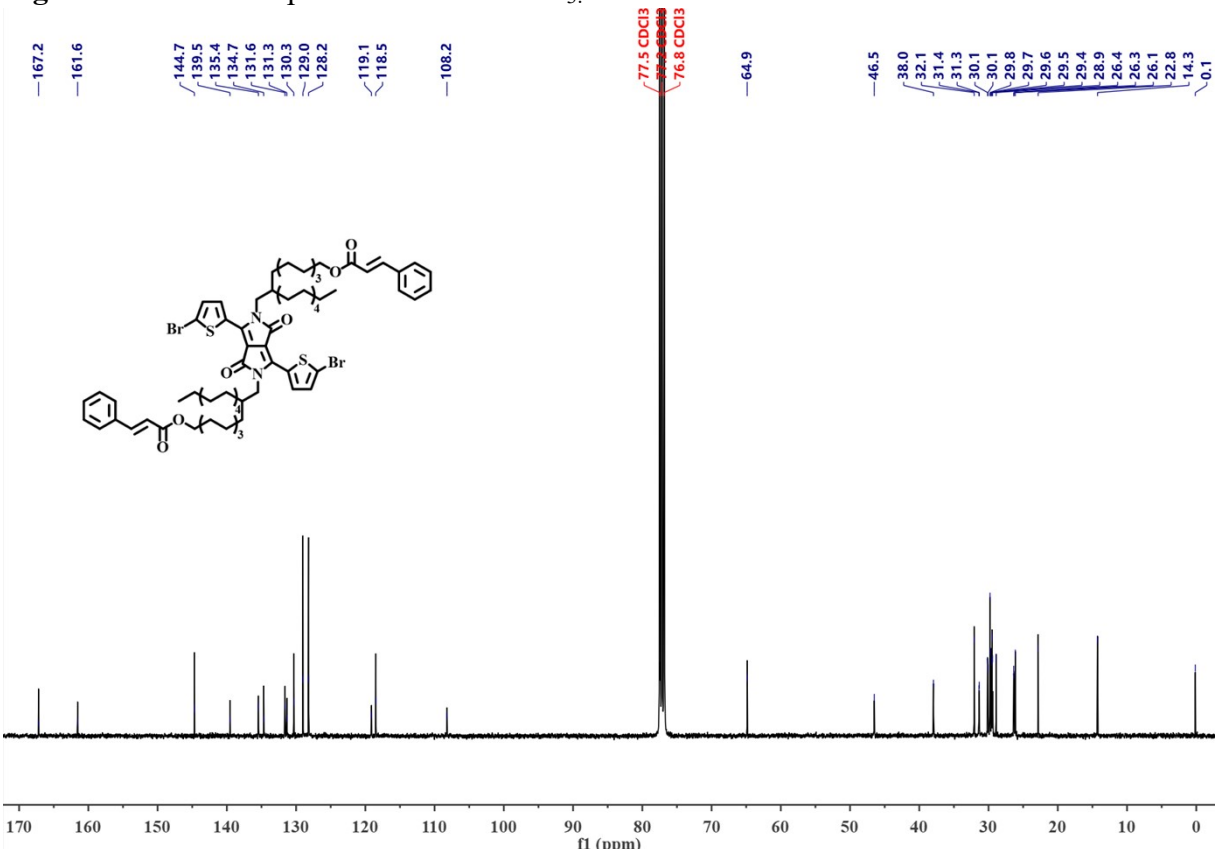

Figure S8. ^{13}C NMR spectrum of **3** in $CDCl_3$.

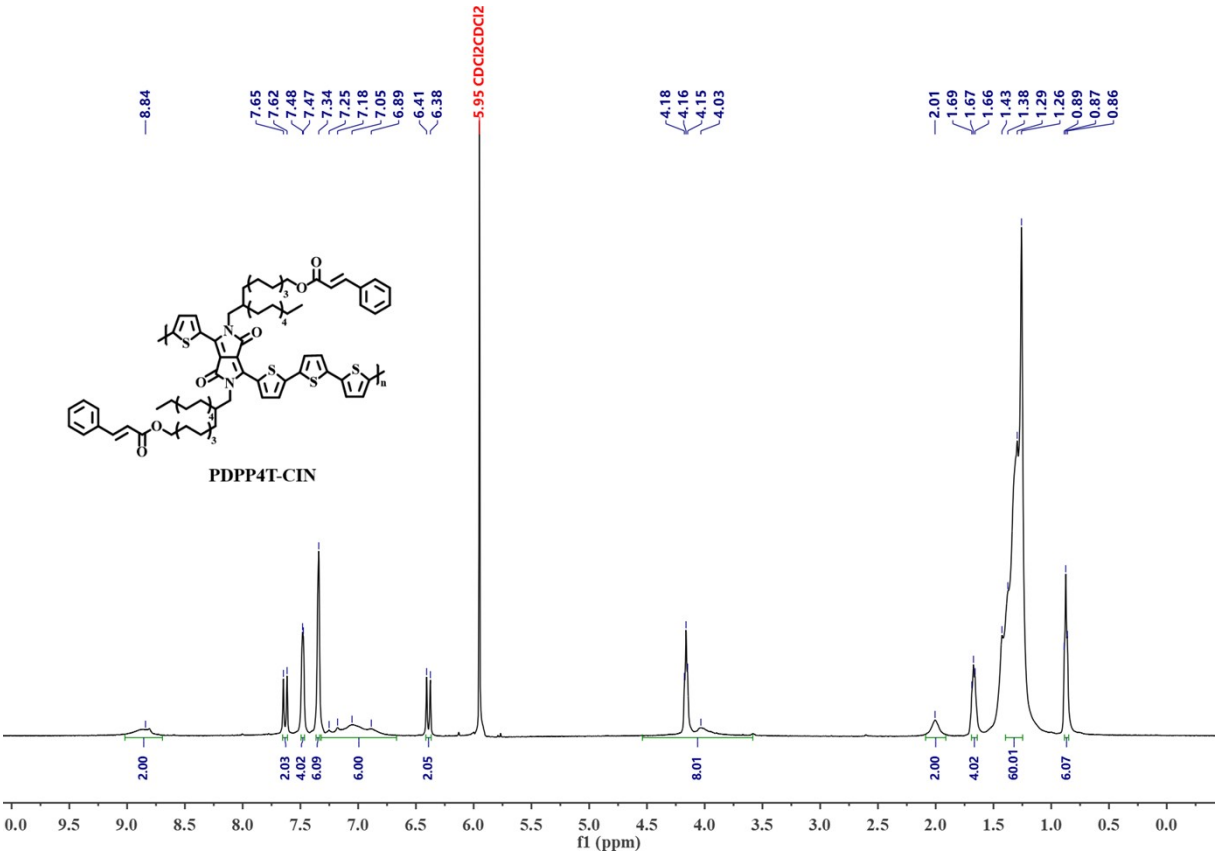

Figure S9. ^{1}H NMR spectrum of **PDPP4T-CIN** in 1,1,2,2-tetrachloroethane-d_2 at 373 K.

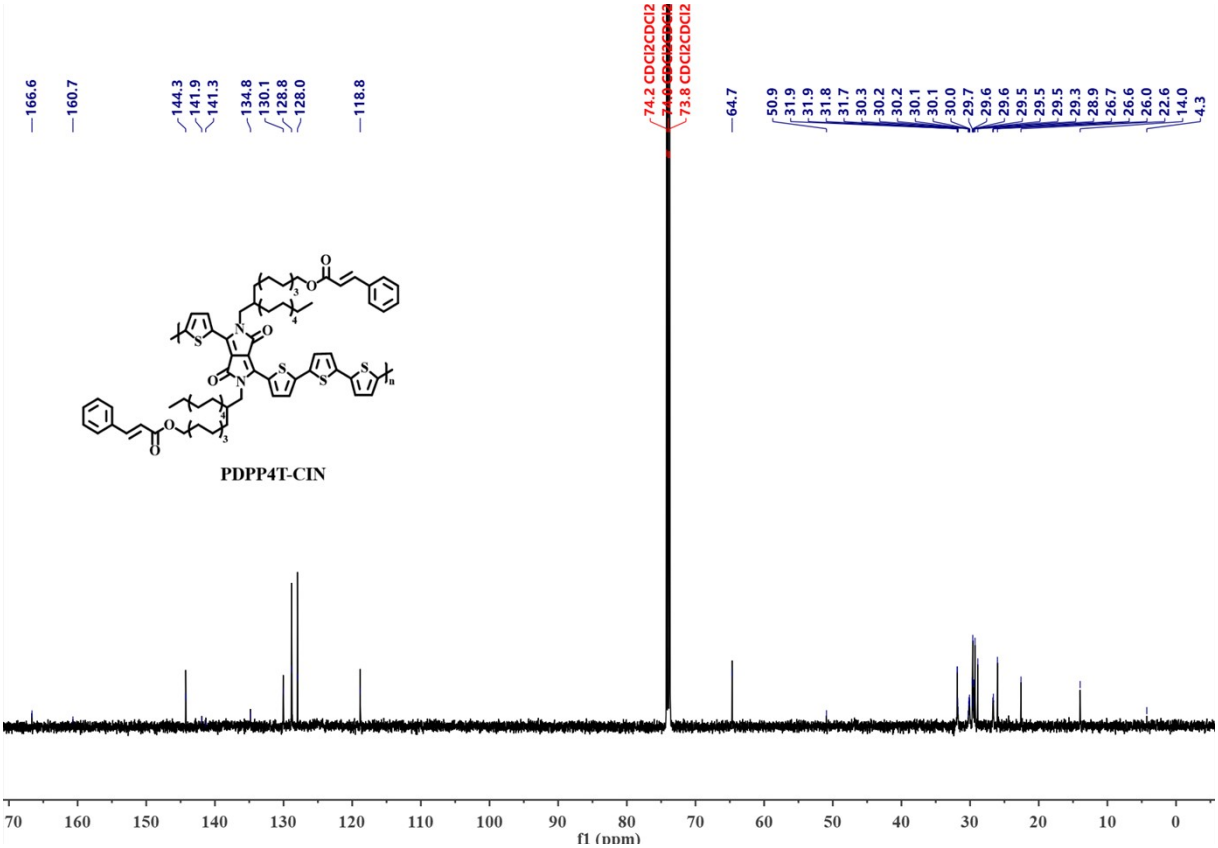

Figure S10. ^{13}C NMR spectrum of **PDPP4T-CIN** in 1,1,2,2-tetrachloroethane-d_2 at 373 K.

12. References

[S1] X. Yu, C. Li, C. Gao, L. Chen, X. Zhang, G. Zhang, D. Zhang, *J. Polym. Sci.* **2022**, 60, 517.

[S2] J. Tian, Z. Liu, W. Jiang, D. Shi, L. Chen, X. Zhang, G. Zhang, C. Di, D. Zhang, *Angew. Chem. Int. Ed.* **2020**, *59*, 13844.